# AUTOMATED MEASURING AND TRACKING THE DEFORMATIONS OF CONCENTRICALLY BRACED FRAMES

*Z. Zhu and L. Tirca
*Concordia University*
*1455 de Maisonneuve West*
*Montreal, Quebec, Canada, H3G 1M8*
*(*Corresponding author: zhenhua.zhu@concordia.ca)*

# AUTOMATED MEASURING AND TRACKING THE DEFORMATIONS OF CONCENTRICALLY BRACED FRAMES

## ABSTRACT

Deformation is a critical indicator required to evaluate the structural safety, stability, and integrity. For example, the deformed shape of a building structure is a key parameter that needs to be measured and tracked during laboratory testing or post-disaster inspections. However, existing techniques used for the deformation measurement and tracking do not have all the desirable characteristics, such as: reliability, accuracy, low-cost and simplicity of tools installation. In order to address this issue, a novel method has been proposed in this study. The method consists on using the image processing technique to automatically measure and track the deformations of concentrically braced frame (CBF) structures. Accordingly, the critical points in a CBF structure are first identified and the topological configuration of the structure is retrieved. The points and topological configuration characterize the basic shape of the structure. In this way, the deformation of the structure can be determined by measuring and tracking these points and their topological configuration. To show its effectiveness, the proposed method has been tested against the manual deformation measurements.

## KEYWORDS

Deformation measurement, CBF structures, Image processing, Automation.

## INTRODUCTION AND RELATED WORK

The deformation of a structure, defined as the alteration of its geometrical shape and initial dimensions, is a critical indicator required to evaluate the structural performance under the applied gravity and earthquake loading. For example, in the aftermath of earthquakes, construction inspectors and/or structural engineers rely on the information of damage, measured as residual deformation, in order to assess the stability of buildings and the level of safety for occupants. (ATC-20, 1989; ATC-20-2, 1995). In addition, monitoring the deformation of structure that is composed of members belonging to the gravity and seismic-force resistant systems, is an important parameter requested to assess the structural integrity of buildings and it provides the basis of knowledge for efficient implementation of building maintenance strategies (Grosso et al. 2011). Moreover, it was found that this long-term monitoring process could help to increase the knowledge of the real behavior of a structure for the purpose of its management and integrity (Inaudi et al. 2001).

There are several techniques that have been adopted to measure the deformation of a structure, including contact sensors, terrestrial laser scanning, etc. The traditional contact sensors (e.g. dial gauges) need to be physically placed on structural elements that are under testing. These sensors could accurately measure small distances and angles. However, their contact nature makes it almost impossible to record a large number of measurements (Gordon and Lichiti 2007). Also, most contact sensors could only capture one-dimensional measurement. Both limitations could be overcome using terrestrial laser scanners, since a terrestrial laser scanner could collect millions of three-dimensional (3D) measurements remotely within minutes. However, the scanner is typically expensive and heavy. Moreover, the 3D measurements captured by the laser scanners were not as accurate as the traditional high-precision sensors. Therefore they are only considered as an useful auxiliary measurement tool (Berenyi and Lovas, 2009). In addition to contact sensors and laser scanner, the use of digital images for the 3D geometric information retrieval (i.e.

photogrammetry) has also been investigated to measure the deformations in a structure (Chen et al. 2011). In the photogrammetry, the 3D deformation is identified from a set of two dimensional (2D) photographic images. Photogrammetry could reach high measurement accuracy. Hence, it was recommended for bridge deformation measuring and structural test monitoring (Jiang et al. 2008) or rapid post-disaster building damage reconnaissance (Dai et al. 2011). However, a lot of manual work is involved, when photogrammetry is used to collect the 3D deformation measurements, including the identification of target points and matching these points in the deformed structure.

The objective of this research work is to facilitate the amount of manual work in the photogrammetry. In order to achieve this objective, a novel method is proposed herein for measuring and tracking the deformations of a concentrically braced frame (CBF) structure from 2D images. Under the method, the images of CBF structure are captured. The images are thresholded and thinned to get the skeleton of the structure. The critical points in the skeleton are identified, and the topological configuration of the structure is retrieved. The points and topological configuration characterize the basic shape of the structure. In this way, the deformation of the structure can be determined by measuring and tracking the critical points and topological configuration of the structure. The proposed method has been tested in a two-storey chevron-bracing office building, located in Victoria, BC. The deformations measured and tracked by the method have been compared with the results obtained from a nonlinear time-history analysis to indicate the effectiveness of the method.

## PROPOSED METHODOLOGY

The proposed method mainly includes four parts:1) image thresholding and thinning, 2) critical point identification, 3) topological configuration retrieval, and 4) tracking. Corner detection is used to identify all the critical connecting and end points in a CBF structure. Then, the topological configuration of the CBF structure is retrieved by creating the necessary links between the critical points. The points plus the topological configuration characterize the basic shape of the CBF structure. Tracking and measuring these points and configuration can help to determine the deformation of the CBF. The overall framework is illustrated in Figure 1. The details are described below.

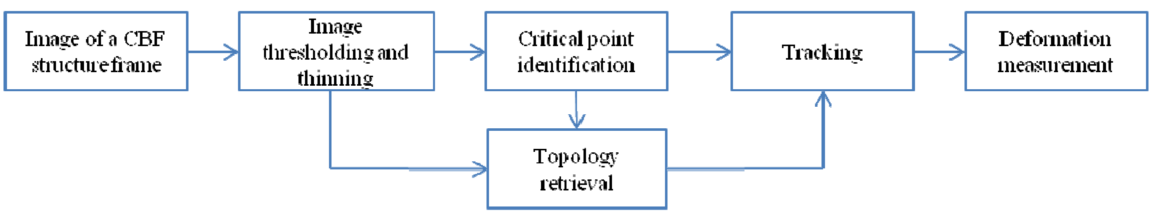


Figure 1 – Framework of the proposed method

### Image Thresholding and Thinning

The first step in the proposed method is image thresholding and thinning. In the thresholding process, the values of the pixels in the image are set equal to zero (black), when their intensities are smaller than the threshold value. Otherwise, their values are replaced with the unity value (white). The purpose of thresholding is to produce a binary (black and white only) image, so that the shape of CBF structure can be extracted from the image background. Herein, the threshold value is selected based on the levels of the image histograms. The selection is decided, when the intra-class variance of the black and white image, given in pixels after thresholding, is minimized (Otsu 1979).

After thresholding, the binary image has been thinned (Lan et al. 1992). The thinning removes unnecessary image pixels on the boundaries of the CBF structure, but does not break the CBF structure apart. In this way, the remaining pixels in the binary image construct a skeleton, which represents a simplified but topologically equivalent version of the CBF structure. The skeleton keeps the important topological properties of the CBF structure, including its connectivity and topological configuration.

**Identification of Critical Points in the CBF structure**

When the image of a CBF structure has been thresholded and thinned, the next step in the proposed method is to identify the critical points in the skeleton of the CBF structure. The critical points are those points that have connecting functions or are at the end positions in the structure. In order to identify these points, the Shi-Tomasi corner detector (Shi and Tomasi 1994) is used. The detector is based on the Harris corner detector (Harris and Stephens 1988) with one slight modification in the "selection criteria" for the corners. This slight modification makes the Shi-Tomasi corner detector work well even when the Harris corner detector (Harris and Stephens 1988) fails.

The Shi-Tomasi corner detector can locate many points of interest where there are large intensity variations (Cooke and WShatmough 2005). However, not all the points of interest located by the Shi-Tomasi corner detector (Shi and Tomasi 1994) are the critical points. Therefore, the points need to be further checked. In doing so, a local window (7x7 image pixels) is placed on each point of interest under the check. The skeleton information in the window is extracted. The point is considered to be a critical point when it meets one of the following two conditions: 1) there are more than two skeleton segments connecting to the point in the local window; or 2) the overall skeleton passing through the point does not cross over the window from one side to another in *x*- or *y*- direction.

**Retrieval of CBF Topological Configuration**

When the critical points are identified, the topological configuration for the skeleton of the CBF structure can be retrieved. A straightforward way is to check the connectivity of any two critical points in the skeleton image. If they are directly connected, it means there is a link between these two points in the topological configuration. However, checking the skeleton connectivity one point by another is time-consuming. This is especially true when the CBF structure is complex (e.g. multiple stories or spans). In addition, it is found that the potential errors in the identification of the critical points may fail the connectivity checking procedure.

In order to address these issues, a new procedure has been proposed here to retrieve the skeleton topological configuration. Specifically, the procedure includes two steps. First, for any pair of critical points, it is assumed that there is a line segment connecting them. The line segment is morphologically 'dilated', and combined with the structure skeleton image using the logic operation, 'and'. If the result after the combination contains a skeleton segment, it means that the assumption is valid and the line segment should be therefore kept. Otherwise, the line segment is discarded. When all possible pairs of critical points are enumerated, the potential line segments connecting the critical points can be identified. These line segments compose a line segments pool. The pool may contain fake line segments (e.g. L1 in Figure 2). In order to remove the fake line segments, any three line segments in the pool that can form a triangle are checked. For each triangle, if the length of its longest side (e.g. L1 in Figure 2) is almost the same as the sum of the length of the other two (e.g. L2 and L3 in Figure2), it means that the line segment representing the longest triangle side can be replaced by the other two. Therefore, it is removed from the pool. For example, in Figure 2, the fake line segment (L1) in the frame was replaced by L2 and L3. After checking all possible triangles, the remaining line segments construct the topological configuration of the frame.

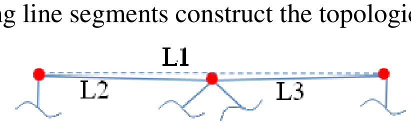


Figure 2 – Removal of fake line segments

**Tracking**

The critical points and the topological configuration of the skeleton characterize the basic shape of the CBF structure. Therefore, the deformation of the structure can be determined by tracking its critical points and topological configuration. Here, tracking is performed by matching the critical points of the structure in consecutive images. First, the positions of the critical points in the images are recorded. For each critical point in image *i*, its Euclidean distances to all the critical points in image *i+1*, are calculated. A critical point in image *i+1* is selected as the best match for that critical point in image *i*, if their Euclidean distance is minimum. This way, the critical points in consecutive images can be matched. The points and the topological configuration can be tracked accordingly.

## IMPLEMENTATION AND RESULTS

### Implementation

The proposed method has been implemented in Matlab R2012a, which can provide the functions for image processing, computer vision, image acquisition, etc. (Mathworks 2012). These functions can facilitate implementing the proposed method. The seismic force resisting system of a two-storey office building located in Victoria, BC was selected for the test. Figure 3 shows the screenshots of using the proposed method. When a CBF structure image prepared by a structural engineer was loaded, the critical points of the structure were identified in Figure 3, and the topological configuration of the structure was retrieved in Figure 4. Herein, Figure 5 illustrated the matching of the points and configuration between the images of the CBF structure under the normal and deformed conditions.

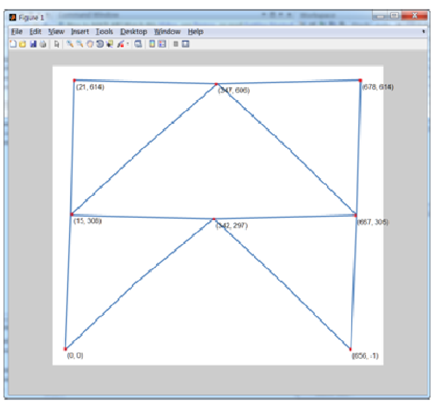


Figure 3 - Critical points identification

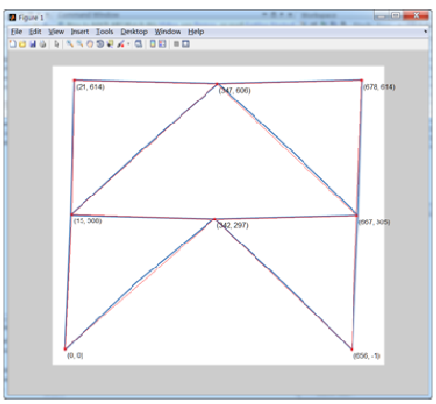


Figure 4 - Topological configuration retrieval

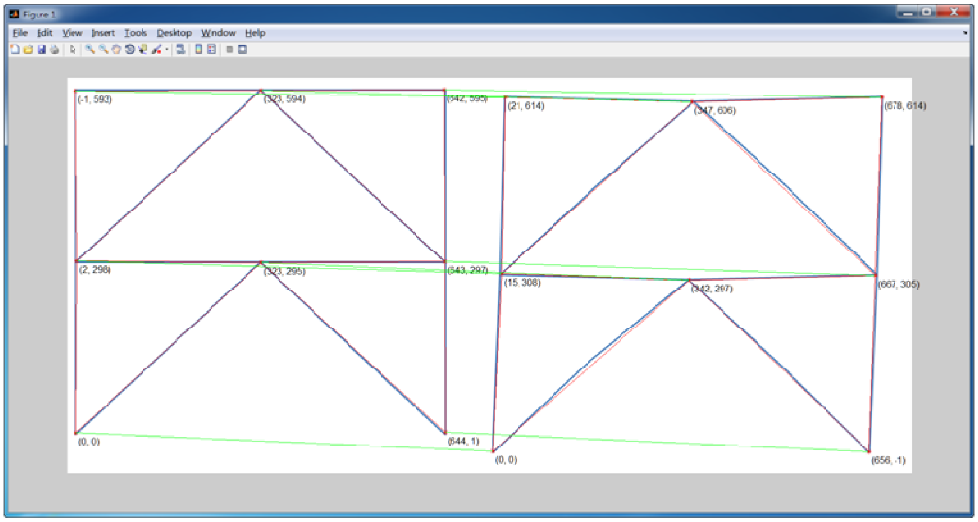


Figure 5 – Tracking of critical points and topological configuration

**Results**

In this paper, the critical points identified by the method were compared with the points in the ground truth to indicate the effectiveness of the method in the identification of critical points. The points in the ground truth were manually identified based on the positions of the structure before and after deformation. Table 1 illustrates the coordinates of points measured by the method. The resolutions of the images before and after the deformation are different. Herein, the point coordinates were normalized. In this example, the normalization used the *x*-distance between points 1 and 6 and the *y*-distance between points 1 and 3 as the reference for *x*- and *y*- normalization separately. Table 2 illustrated the coordinates of the points in the ground truth. The point coordinates in the ground truth were also normalized following the same reference strategy.

Table 1 – Critical point coordinates measured by the method

| No. | Absolute coordinate system (pixels) | | | | Normalized coordinate system | | | |
|---|---|---|---|---|---|---|---|---|
| | Before deformation | | After deformation | | Before deformation | | After deformation | |
| | X | Y | X | Y | X | Y | X | Y |
| 1 | 0 | 0 | 0 | 0 | 0 | 0 | 0 | 0 |
| 2 | 2 | 298 | 15 | 308 | 0.00311 | 0.50253 | 0.02287 | 0.50163 |
| 3 | -1 | 593 | 21 | 614 | -0.0016 | 1 | 0.03201 | 1 |
| 4 | 323 | 295 | 342 | 297 | 0.50155 | 0.49747 | 0.52134 | 0.48371 |
| 5 | 323 | 594 | 347 | 606 | 0.50155 | 1.00169 | 0.52896 | 0.98697 |
| 6 | 644 | 1 | 656 | -1 | 1 | 0.00169 | 1 | -0.0016 |
| 7 | 643 | 297 | 667 | 305 | 0.99845 | 0.50084 | 1.01677 | 0.49674 |
| 8 | 642 | 595 | 678 | 614 | 0.99689 | 1.00337 | 1.03354 | 1 |

Note: the *x*-distance between points 1 and 6 and the *y*-distance between points 1 and 3 are used as the reference for x- and y- normalization separately. The resolution of images captured before and after the deformation is different.

Table 2 – Critical point coordinates in the ground truth

| No. | Absolute coordinate system (mm) | | | | Normalized coordinate system | | | |
|---|---|---|---|---|---|---|---|---|
| | Before deformation | | After deformation | | Before deformation | | After deformation | |
| | X | Y | X | Y | X | Y | X | Y |
| 1 | 0 | 0 | 0 | 0 | 0 | 0 | 0 | 0 |
| 2 | 0 | 3800 | 150 | 3800 | 0 | 0.5 | 0.01974 | 0.5 |
| 3 | 0 | 7600 | 250 | 7600 | 0 | 1 | 0.03289 | 1 |
| 4 | 3800 | 3800 | 3950 | 3700 | 0.5 | 0.5 | 0.51974 | 0.48684 |
| 5 | 3800 | 7600 | 4050 | 7500 | 0.5 | 1 | 0.53289 | 0.98684 |
| 6 | 7600 | 0 | 7600 | 0 | 1 | 0 | 1 | 0 |
| 7 | 7600 | 3800 | 7750 | 3800 | 1 | 0.5 | 1.01974 | 0.5 |
| 8 | 7600 | 7600 | 7850 | 7600 | 1 | 1 | 1.03289 | 1 |

Note: the *x*-distance between points 1 and 6 and the *y*-distance between points 1 and 3 are used as the reference for *x*- and *y*- normalization separately.

After the normalization of the point coordinates, the deformations of the structure could be calculated based on the normalized point coordinates. The calculation results from the method were further compared with the normalized deformation in the ground truth to indicate the effectiveness of the method in the deformation measurement. Table 3 illustrates the deformations calculated from the method and in the ground truth using the coordinates of the points listed in Table 1 and Table 2. Also, the absolute errors in the deformation measurement were included. According to the results given in Table 3, it was found that the average absolute errors for measuring the deformation of the structure in the *x*- and *y*- direction could reach 0.00142 and 0.00173, respectively.

Table 3 – Comparison of the deformation measurements

| No. | Normalized deformation measured by the method | | Normalized deformation in the ground truth | | Absolute errors in the normalized deformation measurements | |
|---|---|---|---|---|---|---|
| | dX | dY | dX | dY | dX | dY |
| 1 | 0 | 0 | 0 | 0 | 0.00000 | 0.00000 |
| 2 | 0.01976 | -0.0009 | 0.01974 | 0 | 0.00002 | 0.00090 |
| 3 | 0.03356 | 0 | 0.03289 | 0 | 0.00067 | 0.00000 |
| 4 | 0.01979 | -0.0138 | 0.01974 | -0.0132 | 0.00005 | 0.00060 |
| 5 | 0.02741 | -0.0147 | 0.03289 | -0.0132 | 0.00548 | 0.00156 |
| 6 | 0 | -0.0033 | 0 | 0 | 0.00000 | 0.00332 |
| 7 | 0.01832 | -0.0041 | 0.01974 | 0 | 0.00142 | 0.00410 |
| 8 | 0.03664 | -0.0034 | 0.03289 | 0 | 0.00375 | 0.00337 |
| Average | | | | | 0.00142 | 0.00173 |

**Discussion**

Although the preliminary results from the experiment are promising, there are certain limitations currently associated with the method. First, the images provided by structural engineers must be the orthogonal projection of the frame. Also, the position and orientation of the camera may produce the perspective distortion, which significantly affects the accuracy of the method. These two limitations could be overcome through camera calibration, which is the pre-requirement of using the proposed method. Once the camera parameters are known from the calibration, the images could be rectified even if the images are not orthogonal. In addition, the results achieved from the method are based on image pixels. It is necessary to convert the pixel-based measurement to the measurement using physical units. In this manner, the absolute accuracy of the method could be evaluated.

## CONCLUSIONS AND FUTURE WORK

Structural engineers always need to measure the deformations of structures in-service to evaluate their stability, safety, and integrity. Considering the importance of deformation measurement, several techniques have been presented to facilitate the measuring process, including traditional contact sensors, digital photogrammetry, terrestrial laser scanning, etc. The benefits of using these techniques have been identified. Meanwhile, it was also noted that existing measuring techniques could not have all desirable characteristics such as: reliability, accuracy, low-cost, etc. In order to address this issue, a novel measuring method has been proposed in this study. The method includes four main parts: 1) image thresholding and thinning; 2) critical point identification; 3) topological configuration retrieval; and 4) tracking. In this way, the deformations of a structure could be determined by automatically measuring and tracking the critical points and topological configuration of the structure with the proposed method. Up to now, the method has been tested in a two-storey office building. The deformation measurements made by the method were compared with the results obtained from the nonlinear time-history analysis, when the building was subjected to crustal ground motions. The obtained results indicate the effectiveness of the method. Future work is required and will focus on overcoming the limitations mentioned above. In addition, in order to validate the method, more examples need to be tested.

## REFERENCES

ATC-20 (1989). "Procedures for Postearthquake Safety Evaluations of Buildings." Report ATC-20, Redwood City, CA.

ATC-20-2 (1995). “Addendum to ATC-20, Procedures for Postearthquake Safety Evaluations of Buildings.” Report ATC-20, Redwood City, California.

Berényi A. and Lovas, T. (2009). "Laser scanning in deformation measurement." GIM International, March 2009: 17-21.

Chen, B.Q., Garbatov, Y., and Guedes Soares, C. (2011). "Automatic approach for measuring deformations in complex structures using photogrammetry technique." In: Proc. of the 22nd Pan American Conference of Naval Engineering, Maritime Transportation, Ports Engineering, Sept. 27-30, 2011, Buenos Aires, Argentina

Dai, F., Dong, S., Kamat, V.R., and Lu, M. (2011). “Photogrammetry assisted measurement of interstory drift for rapid post-disaster building damage reconnaissance.” Journal of Nondestructive Evaluation, 30(3), 201-212. Springer, London, UK”.

Gordon, S. and Lichti, D. (2007). ”Modeling terrestrial laser scanner data for precise structural deformation measurement.” J. Surv. Eng., 133(2): 72–80.

Grosso, A., Inaudi, D., and Cottone, I. (2011). "Measuring deformations of large structural systems." In: Joint International Symposium on Deformation Monitoring, Nov. 2-4, 2011, Hong kong

Inaudi, D., Casanova, N., and Glisic, B. (2001). "Long-term deformation monitoring of historical constructions with fiber optical sensors." In: 3rd International Seminar on Structural Analysis of Historical Constructions, Guimaraes, Portugal, November, pp. 421-430

Lam, L., Lee, S-W., and Suen, C. (1992). "Thining methodologies - a comprehensive survey." IEEE Transactions on Pattern Analysis and Machine Intelligence, 14(9): 869-885

Lightfoot, M., Bruce, G., and Barber, D., (2007). "The measurement of welding distortion in shipbuilding using close range photogrammetry." In: Proc. of the Annual Conference of the Remote Sensing and Photogrammetry Society.

Otsu, N. (1979). "A threshold selection method from gray-level histograms." IEEE Transactions on Systems, Man, and Cybernetics, 9(1): 62-66.

Stanton, J., Eberhard, M., and Barr, P. (2003). "A weight stretched wire system for monitoring deflections." Engineering Structures, 25(3): 347-357.